Fractional and integer angular momentum wavefunctions localized on classical orbits: the case of $E = 0$

2007 J. Phys. A: Math. Theor. 40 11373

(http://iopscience.iop.org/1751-8121/40/37/013)

IOP PUBLISHING JOURNAL OF PHYSICS A: MATHEMATICAL AND THEORETICAL

J. Phys. A: Math. Theor. **40** (2007) 11373–11383 doi:10.1088/1751-8113/40/37/013

Fractional and integer angular momentum wavefunctions localized on classical orbits: the case of $E = 0$

A J Makowski and K J Górska

Institute of Physics, Nicolaus Copernicus University, ul. Grudziądzka 5, 87-100 Toruń, Poland

E-mail: amak@fizyka.umk.pl

Received 2 April 2007, in final form 1 August 2007
Published 29 August 2007
Online at stacks.iop.org/JPhysA/40/11373

Abstract
In two-dimensional space, where the intermediate statistics between bosons and fermions are possible, we study a localization of some stationary coherent states on classical orbits in the potentials $V(r) = -\gamma_\nu/r^\nu$, $\gamma_\nu > 0$ for the total energy $E = 0$. It is shown that excellent quantum-classical correspondence can be reached for two large classes of classical orbits with $\nu < -2$ (open curves) and with $\nu > 2$ (closed curves). To that purpose, it was necessary to introduce fractional angular momenta for some values of ν. They are a consequence of imposing special boundary conditions on the used wavefunctions.

PACS numbers: 03.65.Ge, 45.50.−j, 42.50.Ar

(Some figures in this article are in colour only in the electronic version)

1. Introduction

In recent years, studying relations between quantum mechanics and classical periodic orbits was a subject of growing interest. Among them, constructing wavefunctions perfectly well localized on the orbits seems to be one of the frequently examined problems, especially in mesoscopic systems. Excellent agreement between some coherent states with the above property [1–3] and experimentally generated wave patterns [4, 5] was recently obtained for a variety of Lissajous figures. Also, billiards of various shapes, including circular ones, are examples of physical systems where the correspondence between classical dynamics and quantum probability distributions can be observed formally [6] and experimentally visualized [7]. The wave patterns localized on the periodic orbits of the circular billiards appeared to be represented by some combinations of Bessel-like eigenstates.

We shall show below that similar eigenstates can be found for a wide class of central potentials in the form of $V(r) = -\gamma_\nu/r^\nu$ with $\gamma_\nu > 0$, for both $\nu < -2$ and $\nu > 2$. Their general discussion in the 3D space, also including the cases for $-2 \leqslant \nu \leqslant 2$, is given in the Landau and Lifshitz's handbook [8]. Next, we shall show how to construct a coherent state well localized on any of the classical orbits related to the potentials.

We should point out that though all the potentials are unbounded from below, some of them have found physical applications. Examples can be tracked down in collision theory [9], molecular [10] and chemical [11] physics and also in vortex lattices [12].

For a number of reasons, the above potentials are studied in the case of $E = 0$ only. Thus, we can examine interrelations between the classical and quantum mechanics and its classical limit in the most interesting region of energies. Besides, the $E = 0$ states have been applied to the cold-atom collisions [13, 14], to the quantum cosmology problems [15] and to the description of some vortex lattices [12].

Since for the central potentials, the angular momentum is a conserved quantity, all classical trajectories are flat and, consequently, we may restrict ourselves to the 2D space. As we will see later on, the dimensionality plays a crucial role in producing some unusual properties of the localized states proposed here. Moreover, to have the quantum probability densities assuming the shape of the classical trajectories corresponding to them, some non-trivial boundary conditions have to be imposed on the used wavefunctions for the potentials $V(r) = -\gamma_\nu/r^\nu$. In consequence, fractional angular momenta may appear and this is what makes the study very interesting.

2. Classical orbits

We shall present first the exact classical solutions for the central potentials $V(r) = -\gamma_\nu/r^\nu = -\gamma_\nu/r^{2\mu+2}$, where $\gamma_\nu > 0$, $-\infty < \nu < \infty$, $\mu = (\nu - 2)/2$ and $r = \sqrt{x^2 + y^2}$. The simplest way of deriving the solutions consists in using the polar coordinates (r, φ) and then the conservation laws for energy and angular momentum. Thus, we have

$$0 = T + V = (m/2)\dot{\varphi}^2[(\mathrm{d}r/\mathrm{d}\varphi)^2 + r^2] + V(r) \tag{1}$$

$$L = L_z = mr^2\dot{\varphi} \tag{2}$$

where the dot over φ stands for the time derivative and all the classical orbits lie on the (x, y) plane. Now, introducing the dimensionless position

$$\rho = r/a_c \tag{3}$$

with

$$a_c \equiv (2m\gamma_\nu/L^2)^{1/(2\mu)} = (2m\gamma_\nu/L^2)^{1/(\nu-2)} \tag{4}$$

where $\mu \neq 0$ and $\nu \neq 2$, we get the following equation for trajectories:

$$\left(\frac{\mathrm{d}\rho}{\mathrm{d}\varphi}\right)^2 + \rho^2 = \rho^{4-\nu} = \rho^{2-2\mu}. \tag{5}$$

Its general solution is well known [16] and reads

$$r^\mu = a_c^\mu \cos[\mu(\varphi - \varphi_0)]. \tag{6}$$

Equation (6) represents a variety of bound curves for $\nu > 2$ $(\mu > 0)$ which all lie on and inside the circle $r = a_c$ $(\rho = 1)$. The cardioid $(\mu = 1/2, \nu = 3)$, the circle $(\mu = 1, \nu = 4)$, the Bernoulli lemniscate $(\mu = 2, \nu = 6)$ and for $\mu = n$ $(\nu = 2n + 2)$ with $n = 3, 4, 5, \ldots,$ the roses made up of n petals are the examples. For an arbitrary initial angle φ_0, the classically allowed area is given by the condition $r \leqslant a_c$ $(\rho \leqslant 1)$. When φ_0 assumes a fixed value, for example $\varphi_0 = 0$, as in the figures below, the area shrinks to one or several sectors.

Meanwhile, all the curves for $\nu < 2$ ($\mu < 0$) are unbounded and lie on and outside of the circle $r = a_c$. Again, the classically allowed area, $r \geqslant a_c$, shrinks to some sectors when φ_0 is fixed.

The value of $\nu = 2$ ($\mu = 0$) represents the borderline between the bound and unbound solutions. The orbits with $-2 \leqslant \nu \leqslant 2$ are excluded from our study since the wavefunctions corresponding to them are now not square-integrable [17, 18].

3. Quantum solutions

Having found the $E = 0$ classical solutions, we can obtain now their exact quantum 2D counterparts. For the class of potentials under consideration, the angular and radial parts of wavefunctions can be easily separated and there is enough to solve the following radial equation:

$$\left[\frac{-\hbar^2}{2m}\left(\frac{\partial^2}{\partial r^2} + \frac{1}{r}\frac{\partial}{\partial r} - \frac{l^2}{r^2}\right) - \frac{\gamma_\nu}{r^\nu}\right] R_l(r) = 0 \tag{7}$$

where l is to be specified later. It is worth to introduce the dimensionless variable ρ, as in the classical case, in the form

$$\rho = r/a_q \tag{8}$$

where a_q is, of course, a quantity of the dimension of length. Changing additionally the independent variable as $z = 1/\rho$, we obtain

$$\left(z^2\frac{\mathrm{d}^2}{\mathrm{d}z^2} + z\frac{\mathrm{d}}{\mathrm{d}z} - l^2 + g^2 z^{\nu-2}\right) R_l(z) = 0 \tag{9}$$

where

$$g^2 \equiv \frac{2m\gamma_\nu}{\hbar^2 a_q^{\nu-2}} \tag{10}$$

and, obviously, g is a dimensionless quantity as well.

Square-integrable solutions of equation (9) are given in terms of the Bessel functions of the first kind [17, 18]

$$R_l(z) = N_l J_{\frac{l}{|\mu|}}\left(\frac{g z^\mu}{|\mu|}\right) \tag{11}$$

with the normalization constant

$$N_l = \sqrt{\frac{2\sqrt{\pi}|\mu|}{a_q^2}\left(\frac{|\mu|}{g}\right)^{2/\mu}\frac{\Gamma(1+1/\mu)\Gamma(1+l/|\mu|+1/\mu)}{\Gamma(1/2+1/\mu)\Gamma(l/|\mu|-1/\mu)}}, \tag{12}$$

if l and μ obey the conditions

$$\frac{2l}{|\mu|} + 1 > \frac{2}{\mu} + 1 > 0. \tag{13}$$

Thus, two classes of solutions emerge. For $\nu > 2$ ($\mu > 0$), the functions $R_l(z)$ correspond to bound states if $l > 1$, and the classical solutions of equation (6) are closed orbits. When $\nu < -2$ ($\mu < -2$), the functions $R_l(z)$ are still normalizable if $l \geqslant 0$, and the classical orbits corresponding to them are open curves. In this case, the quantum solutions cannot be considered as bound states.

4. Fractional angular momentum

We shall now comment on the allowed values for the angular momentum quantum number l. It follows from the results of the previous section that the complete normalized wavefunctions can be written in the explicit form as

$$\Phi_{\mu,l}(r,\varphi) = N_\varphi \exp(\mathrm{i}l\varphi) N_l J_{\frac{l}{|\mu|}}\left(\frac{g a_q^\mu}{|\mu| r^\mu}\right) \tag{14}$$

where N_φ is a normalization factor in the angle variable. From conditions (13) it follows, in turn, that with given μ the value of l has to be such that it obeys the conditions only. Besides, it may be an arbitrary quantity, e.g., not necessarily integer or half-integer.

At first sight, it seems to be not acceptable on physical grounds. After all, in every textbook on quantum mechanics the requirement of a singlevaluedness of wavefunctions is one of the basic ones. It has at least two important consequences. First of all, the wavefunction has to be 2π-periodic, i.e., $\psi(r,\varphi) = \psi(r,\varphi + 2\pi)$ which leads to integer values of l only. Thus, the orbital angular momentum is quantized in the well-known standard way and the wavefunctions are single-valued. Also, the requirement that the wavefunction is single-valued and continuous leads to the quantization of vortices around wavefunctions nodes [19]. We should, however, emphasize at this point that all this is only true in three- or higher-dimensional space.

In general, as noticed for example by Wilczek [20]: ... *in three spatial dimensions the angular momentum can only be integer or half-integer, ... in two-dimensional situation more possibilities open up, both for the spin and for the statistics*. In this connection, some additional comments on allowed values of l in 2D space are in order.

In quantum mechanics, the orbital angular momentum can be introduced in two equivalent ways: (i) by the relation $\mathbf{L} = \mathbf{r} \times \mathbf{p}$ with $\mathbf{p} = -\mathrm{i}\hbar\nabla$ and (ii) as a generator of an infinitesimal rotation by the angle φ, say $1 - (\mathrm{i}/\hbar)\delta\varphi(xp_y - yp_x)$.

In the 3D or higher-dimensional space, this leads to integer or half-integer values of the angular momentum. In the 2D case, the above two ways fail and the orbital angular momentum is ambiguous by an additive constant. This is so because the rotation group $SO(2)$ in 2D space does not give a unique prescription for the angular momentum [21]. Since the group is parametrized by a single angle, hence the group manifold consists of the points on circle. Then, the function $\exp(\mathrm{i}l\varphi)$ is single-valued if l is an integer, and otherwise it is multi-valued.

The points on the circle form, in the latter case, a multiply connected space. Even in such a case, the functions $\exp(\mathrm{i}l\varphi)$ can also be made single-valued in 2D space [21] if the new group is constructed with $x \to \varphi = x - 2\pi[x/2\pi]$, $-\infty < x < \infty$, $0 \leqslant \varphi \leqslant 2\pi$, where the symbol $[x/2\pi]$ means the largest integer less than $x/2\pi$. All this is an origin of the statistics intermediate between bosons and fermions.

To the best of our knowledge, the earliest comprehensive study of the connection between the dimensionality of space and the quantum statistics was done in [22]. Authors of the cited work have shown with full particulars, for quadratically integrable functions defined on the classical configuration space, that in 1D and 2D spaces intermediate statistics between bosons and fermions are possible. Related to them angular momenta do not need to be integers.

As also noticed in [23], if one considers problems with excluded regions of space, as in our work, there is no singlevaluedness requirement on the wavefunction and the angular momentum may take arbitrary values.

In another study [21], based on the path-integral approach, the fractional angular momentum quantization was a result of an existence of some non-trivial representation of the fundamental group in 2D multiply connected spaces.

We should also point out that the 2D space of coordinates in quantum mechanics may be multiply connected. The reason is that all wavefunctions, except for some special cases, have nodes i.e. the points where $\psi = 0$. For them the observable $|\psi(x, y)|^2$ is exactly zero and the points are excluded for the particle to be found there. Thus, a closed loop shrinks to a point only if the loop in the 2D space does not encircle a nodal point. In consequence, the 2D space has to be multiply connected and, as shown in [21, 23], fractional angular momenta are a natural result of the fact.

In the 3D space, the loop encircling the node can always be deformed in such a way that it can be shrunk to a point. So in the 3D space, except perhaps for some problems in the electromagnetic field, like the Aharonov–Bohm effect, we deal only with simply connected spaces and the fractional angular momenta do not appear.

Summing up the results quoted so far, we may ascertain that fractional angular momenta are a very general feature of 2D systems. Related to them are exotic statistics, intermediate between bosons and fermions. A model-independent formal proof of the fact, based on the path-integral formulation, is given in [24]. It introduces the so-called θ statistics which interpolate between the Bose–Einstein ($\theta = 0$) and Fermi–Dirac ($\theta = \pi$). A similar result was obtained earlier [22] by consideration of the configuration space of a system of identical particles. In that case, the statistics were distinguished by the parameter η with $\eta = 0$ for bosons and $\eta^{-1} = 0$ for fermions.

Fractional angular momentum quantum numbers appear in many important physical applications. Perhaps, the best known example is the mentioned Aharonov–Bohm effect [20, 23, 25]. Some other examples include an application to the cosmic string in spacetime [26], a two-vortex system in a superfluid film [27], necklace-ring solitons [28, 29], a chiral p-wave superconductor [30] or a quantum billiard [31] inside a boundary defined by a wedge-shaped section of a circle.

In the present study, arbitrary values of the angular momentum l in equation (14) follow directly from non-trivial boundary conditions we impose on the angular part of the wavefunctions and can be justified by the topology of the two-dimensional space. Additionally, the prescription for their explicit values will be given from the requirement that the classical and quantum scales of length are the same.

We shall now introduce an unusual periodicity in the azimuthal variable which results in using the following non-trivial boundary conditions for the solutions in equation (14):

$$\Phi_{\mu,l}(r, \varphi) = \Phi_{\mu,l}(r, \varphi + 2\pi/|\mu|). \tag{15}$$

Hence, requiring regular solutions in the φ variable, we obtain

$$l = c + n|\mu| \tag{16}$$

where $n = 0, \pm 1, \pm 2, \ldots$, and $c/|\mu|$ is an integer, while for c the value of 2 is accepted in accordance with condition (13). With the choice for l, the wavefunction is invariant under the transformation (15).

On the other hand, the source of relation (15) and arbitrary values of l in equation (16) lie formally in the necessity of imposing the μth-order symmetries on the quantum probability distributions in order to get the latter arranged along the suitable classical orbits. Similar boundary conditions were used, for example, in applications to cosmic strings [26] and to a description of the Aharonov–Bohm effect [32].

Physical grounds for the benefit of the periodicity (15), and consequently fractional angular momenta (16), may be given via dimensionality arguments of the used space.

In the 3D situation this problem is quite simple and well resolved. Namely, we accept 2π-periodicity, i.e., $\psi(r, \varphi) = \psi(r, \varphi + 2\pi)$ which results, for the orbital angular momentum, in the integer and half-integer quantum numbers only. The latter values are considered to be not acceptable. Two most popular arguments advanced against half-integers are (i) the function $\exp(\mathrm{i}l\varphi)$ would acquire a minus sign under a 2π rotation for such l's. Thus, the total wavefunction would not be single-valued and we need a $\varphi = 4\pi$ rotation to get back to the same state which, however, does not constitute any serious problem (see below) and (ii) the spherical harmonics $Y_{l,m}(\theta, \varphi)$ would become singular for some values of θ and such would be the wavefunction as well. That is why the standard quantization procedure leads in the 3D case to only integer values for the orbital angular momentum quantum numbers.

In the 2D case, the choice of the proper quantum numbers for the angular momentum is not so clear as above and, for a number of reasons, can be considered as a much more subtle task than in the 3D situation. Firstly, there is not any trouble now with the singularity in the angle variable. The only question that remains is the singlevaluedness of the wavefunctions. However, we can argue after [33] that the wavefunction, say $\psi(r, \varphi)$, does not have any direct physical significance as an observable. This is in contrast, for example, to the classical electromagnetism where the field is a physical observable. Moreover, the physical meaning is attributed to quantum averages such as $\langle\psi|\hat{O}|\psi\rangle$ and not to ψ itself. Hence, the averages remain unchanged even if the wavefunction ψ changes sign under a rotation which is the case when angular momentum quantum numbers are not integers. Secondly, as we have already mentioned earlier in this section, the standard ways of defining angular momentum fail in the 2D space.

Taking all this into account and observing that no physical principles rule out arbitrary periodicity of wavefunctions in 2D space, we have proposed it in the form of equation (15) which is best suited for our quantum-classical comparisons.

5. States localized on classical orbits

The states that are localized on the classical solutions (6) are proposed in the following form:

$$\Psi_{\mu,N}(r, \varphi, \tau) = \frac{1}{(1+|\tau|^2)^{N/2}} \sum_{k=0}^{N} \binom{N}{k}^{1/2} \tau^k \Phi_{\mu,c+k|\mu|}(r, \varphi). \tag{17}$$

The pre-factor in equation (17) follows from the normalization of the function to unity, τ is a complex parameter equal to $\tau = A\exp(\mathrm{i}\phi)$ and N_φ of equation (14) reads $N_\varphi = (2\pi/|\mu|)^{-1/2}$. Both Φ and Ψ are regular functions of their arguments and when $\mu > 0$ ($\nu > 2$) they go to zero as $r = 0$ and are finite as $r \to \infty$. In the case of $\mu < -2$ ($\nu < -2$) the functions tend to zero as $r \to \infty$ and are finite at $r = 0$.

As we have discussed in detail elsewhere [34], the state like that in equation (17) obeys all requirements to be called coherent. We have also pointed out there a possible way of its derivation.

We are now ready to examine the quantum-classical correspondence by comparing the images of $|\Psi_{\mu,N}|^2$ and the related classical trajectories. Since the simpler case of integer values of l has already been discussed [34], we are mostly concentrated here on the images with fractional l's.

To have the correspondence as exact as possible, we require the trajectories to be running over the apogees of the quantum probability distributions for arbitrary μ and other parameters. To this end, let us first note that from equations (4) and (10), we get

$$L^2 = g^2\hbar^2 \left(\frac{a_q}{a_c}\right)^{\nu-2} \tag{18}$$

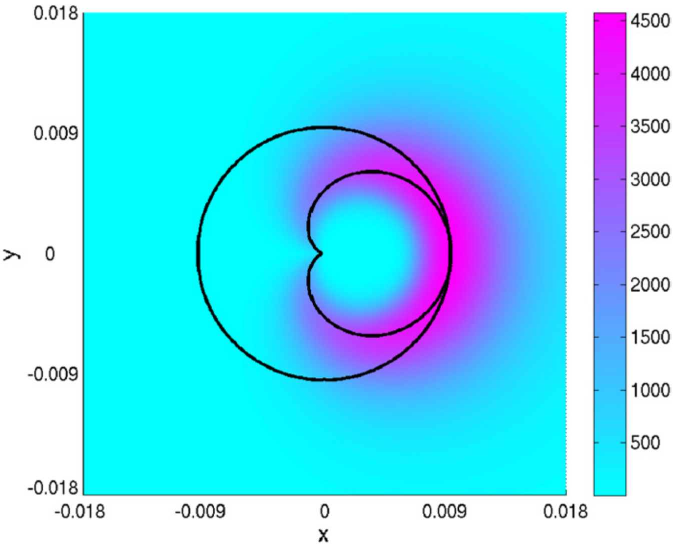

Figure 1. Probability density $|\Psi_{\mu,N}(r,\varphi,\tau)|^2$ and the corresponding *closed* classical orbit, together with the circle of the radius $g^{-1/\mu}$ for $\varphi_0 = \phi = 0$, $A = 1$, $\alpha = 1.30$, $N = 30$, $c = 3/2$ and $\mu = 1/2$ ($\nu = 3$). The coherent state $\Psi_{\mu,N}(r,\varphi,\tau)$ is a combination of 31 degenerated *bound* states of energy $E = 0$. Dimensionless units are used as explained in the text.

where L is the classical angular momentum. The so far undetermined dimensionless quantity g can be derived from the relation

$$\langle\hat{L}\rangle + \alpha\hbar = L \tag{19}$$

with $\hat{L} = -\mathrm{i}\hbar\partial/\partial\varphi$ and the quantum average is taken in the state (17). Since both φ_0 and ϕ rotate only the classical and the quantum images, respectively, by the same angle, we take $\varphi_0 = \phi = 0$. Now, after some calculations, we can show that $\langle\hat{L}\rangle = \hbar[c + |\mu|NA^2/(1+A^2)]$, and from equations (18) and (19) we have

$$g = \left(\frac{a_c}{a_q}\right)^{\mu}\left(c + \frac{|\mu|NA^2}{1+A^2} + \alpha\right). \tag{20}$$

The symbol α represents a correction necessary to balance the classical and quantum angular momenta.

It is justified in the context of our work to assume equality of both length scale factors a_c and a_q. Note that a_c for $\nu > 2$ can be related to the radius at which the effective potential $L^2/2mr^2 - \gamma_\nu/r^\nu$ vanishes, and, in the case of $\nu < -2$, to the distance of closest approach. Thus, according to equation (18), the classical angular momentum is non-integer multiple of the Planck's constant, i.e.

$$L^2 = g^2\hbar^2. \tag{21}$$

Figures 1–4 are now drawn using $\sqrt{2m\gamma_\nu/\hbar^2} = 1$ and, consequently, $a_c^\mu = 1/g$ in equation (6), $a_q^2 g^{2/\mu} = 1$ in equation (12), $g a_q^\mu = 1$ in equation (14) where, in the definition of g in equation (20), we have $a_c = a_q$. Next, we select a central potential by fixing the value of μ and we plot the circle $r^\mu = (x^2+y^2)^{\mu/2} = 1/g$, the classical orbit from equation (6) and the quantum probability density $|\Psi_{\mu,N}(r,\varphi,\tau)|^2$ from equation (17).

Our numerical tests show that surprisingly the probability densities obtained from equation (17) assume the precise shapes of the classical curves from equation (6) for *all*

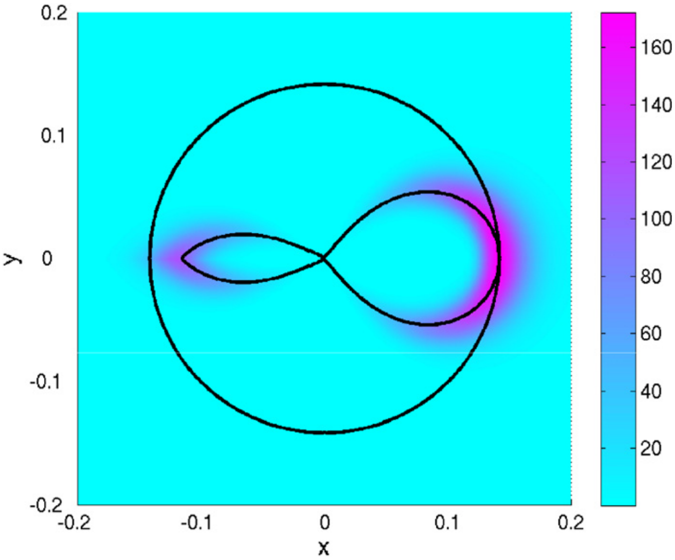

Figure 2. As in figure 1 but for $\mu = 7/4$ ($\nu = 11/2$), $\alpha = 2.67$ and $c = 7/4$.

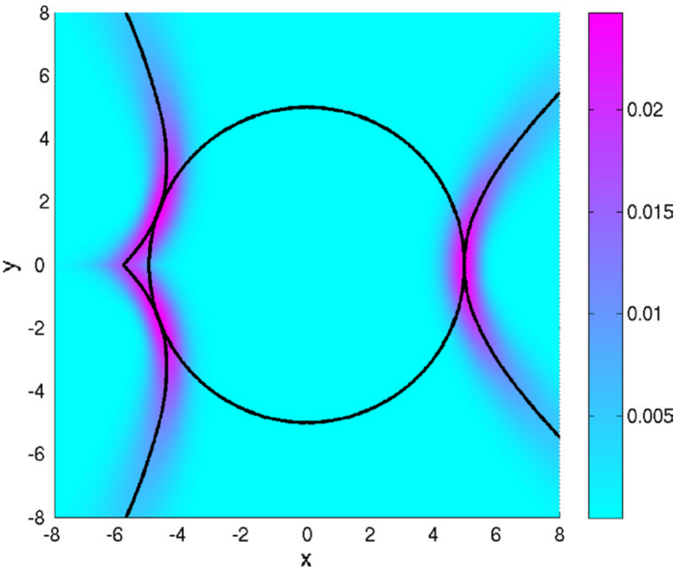

Figure 3. Probability density $|\Psi_{\mu,N}(r, \varphi, \tau)|^2$ and the corresponding *open* classical orbit, together with the circle of the radius $g^{-1/\mu}$ for $\varphi_0 = \phi = 0$, $A = 1$, $\alpha = 1.22$, $N = 30$, $c = 9/4$ and $\mu = -9/4$ ($\nu = -5/2$). The coherent state $\Psi_{\mu,N}(r, \varphi, \tau)$ is constructed now from 31 degenerate *unbound* states of energy $E = 0$.

values of $\nu > 2$ ($\mu > 0$) and $\nu < -2$ ($\mu < -2$). However, to get the shapes in the same scale, i.e., the classical orbits running exactly over the apogees of the quantum probabilities, it is necessary to adjust the value of α in each case. We have done this in the following way. First, we fix the value of c and calculate max $|\Psi_{\mu,N}(x > 0, y = 0, \tau)|^2$. From this, the value of $1/g$ follows. Then, the best fit for α can be found from equation (20).

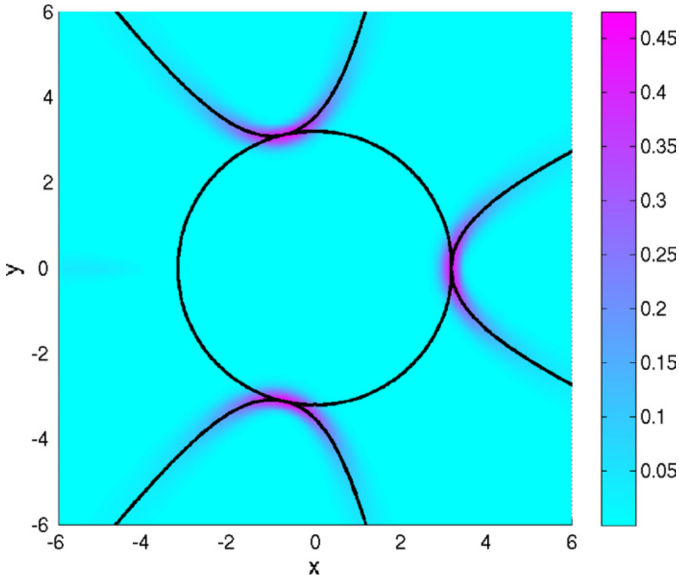

Figure 4. As in figure 3 but for $\mu = -7/2$ ($\nu = -5$), $\alpha = 2.46$ and $c = 7/2$.

The agreement between the classical and quantum images is not very sensitive to the precise values of the parameter. It is also the case for the value of N. It appears that merely few terms in equation (17) are enough to get acceptable localization of the probability density on the classical orbits. This is quite surprising especially for $\nu < -2$ ($\mu < -2$) where closed classical orbits do not exist and the quantum states, though square-integrable, do not represent bound states.

It is worth pointing out that the images 1–4 can also be obtained for other sets of l. For example, l in figure 1 takes the values (cf equation (16)) $l = 3/2, 3/2+1/2, 3/2+1, 3/2+3/2$ and so on. Instead, we might use $l = 2 + k$ with $k = 0, 1, 2, \ldots$ to obtain again the same figure. The values of l used in figures 1–4 follow from the symmetries of the classical figures in each particular case. The worked out examples show that in the 2D space the values of angular momentum can be arbitrary in contrast to the case of the 3D or higher-dimensional spaces where it is allowed to be only integer or half-integer.

Both for the closed orbits like those in figures 1 and 2 and for the open ones like those in figures 3 and 4, the region in and around the origin of coordinates has the probability density being practically equal to zero. This is so because the Bessel functions in equation (17) all vanish as $r = 0$ and $r \to \infty$.

As the last but not least point of this section, it is worth to note that the above described procedure of adjusting classical curves to the related quantum probability distributions is not unique. The reason is the scaling property [17] of the power-law potentials $V(r) = -\gamma_\nu/r^\nu = -g^2\varepsilon_0 a_q^\nu\big/r^\nu$, where g^2 is given in equation (10) and $\varepsilon_0 \equiv \hbar^2\big/2ma_q^2$. Namely, they do not have a built-in length scale and we can change the value of g^2 by a positive factor, to $\sigma^2 g^2$, which changes $g \to \sigma g$ in equation (12) and the argument of the wavefunction in equation (14) to $\sigma g a_q^\mu\big/|\mu| r^\mu$, i.e., it causes a change of the length scale only. That is why the solutions (14) exist for arbitrary coupling constants $g^2 > 0$.

In such a case, the plots of $|\Psi_{\mu,N}(r,\varphi,\tau)|^2$ and the suitable classical orbits can also be well-fitted by putting $\alpha = 0$ into equations (19) and (20) and adjusting only the values of σ.

This can easily be done and figures 1–4 are reproduced once more if $\sigma = 0.87, 0.91, 0.97, 0.96$, respectively.

6. Conclusion

We have demonstrated here the perfect agreement between classical orbits and quantum probability distributions for the large class of central potentials. The quantum-classical correspondence was obtained with the help of some stationary coherent states which differ from the standard ones in that the latter usually represent a wave packet 'following' the classical orbit. To that purpose, it was necessary to impose special boundary conditions on the used quantum solutions. As a result, fractional angular momenta appeared which were proved in the literature to be acceptable when the dimensionality of the space $D = 2$ [35]. This work extends the class of problems mentioned in section 4 where such angular momenta are justified.

We should also mention at this point that in quantum mechanics, except for the above effect of dimensionality, there is always another one [17], independent of the assumed boundary conditions. Namely, the value of D enters the Schrödinger equation in two places. The first is due to the operator $(D-1)(1/r)(\partial/\partial r)$ and the second one is in the quantity $l(l+D-2)/r^2$, which in our case of $D = 2$ represents the second and the third terms in equation (7), respectively.

Let us additionally note that fractional angular momenta can be related to the central potentials $V(r) = -\gamma_\nu/r^\nu$ not only with even but also with odd and fractional powers ν. Even in the latter case, the potentials were the subject of interest [36, 37] and found applications as phenomenological potentials in the nuclear and particle physics.

Acknowledgments

We wish to thank the referee for valuable suggestions and drawing our attention to the papers [24, 35].

References

[1] Chen Y F and Huang K F 2003 *J. Phys. A: Math. Gen.* **36** 7751
[2] Makowski A J 2005 *J. Phys. A: Math. Gen.* **38** 2299
[3] Górska K J, Makowski A J and Dembiński S T 2006 *J. Phys. A: Math. Gen.* **39** 13285
[4] Chen Y F, Lan Y P and Huang K F 2003 *Phys. Rev.* A **68** 043803
[5] Chen Y F, Huang K F and Lan Y P 2003 *Opt. Lett.* **28** 1811
[6] Lee S Y, Rim S, Ryu J W, Kwon T Y, Choi M and Kim C M 2004 *Phys. Rev. Lett.* **93** 164102
[7] Chinnery P A and Humphrey V F 1996 *Phys. Rev.* E **53** 272
[8] Landau L D and Lifshitz E M 1958 *Quantum Mechanics, Non-Relativistic Theory* (Reading, MA: Addison-Wesley) chapters 18 and 35
[9] Joachain C J 1983 *Quantum Collision Theory* (Amsterdam: North-Holland)
[10] Child M S 1998 *J. Phys. A: Math. Gen.* **31** 657
Vogt E and Wannier G H 1954 *Phys. Rev.* **95** 1190
[11] Child M S 1967 *Mol. Phys.* **12** 401
[12] Kobayashi T 2002 *Physica* A **303** 469
[13] Sadeghpour H R, Bohn J L, Cavagnero M J, Esry B D, Fabrikant I I, Macek J H and Rau A R P 2000 *J. Phys. B: At. Mol. Opt. Phys.* **33** R93
[14] Wang H, Wang X T, Gould P L and Stwalley W C 1997 *Phys. Rev. Lett.* **78** 4173
[15] Nowakowski M and Rosu H C 2002 *Phys. Rev.* E **65** 047602
[16] Daboul J and Nieto M M 1995 *Phys. Rev.* E **52** 4430
[17] Daboul J and Nieto M M 1994 *Phys. Lett.* A **190** 357

[18] Daboul J and Nieto M M 1996 *Int. J. Mod. Phys.* A **11** 3801
[19] Hirschfelder J O, Goebel C J and Bruch L W 1974 *J. Chem. Phys.* **61** 5456
[20] Wilczek F 1982 *Phys. Rev. Lett.* **48** 1144
Wilczek F 1982 *Phys. Rev. Lett.* **49** 957
[21] Liang J Q and Ding X X 1987 *Phys. Rev.* A **36** 4149
Schulman L 1968 *Phys. Rev.* **176** 1558
Hamermesh M 1962 *Group Theory* (Reading, MA: Addison-Wesley) p 320
[22] Leinaas J M and Myrheim J 1977 *Nuovo Cimento* B **37** 1
[23] Jackiw R and Redlich A N 1983 *Phys. Rev. Lett.* **50** 555
[24] Wu Y-S 1984 *Phys. Rev. Lett.* **52** 2103
[25] Liang J Q 1984 *Phys. Rev. Lett.* **53** 859
[26] Coelho J L A and Amaral R L P G 2002 *J. Phys. A: Math. Gen.* **35** 5255
[27] Leinaas J M and Myrheim J 1988 *Phys. Rev.* B **37** 9286
[28] He Y J, Fan H H, Dong J W and Wang H Z 2006 *Phys. Rev.* E **74** 016611
[29] Desyatnikov A S and Kivshar Y S 2001 *Phys. Rev. Lett.* **87** 033901
[30] Goryo J 2000 *Phys. Rev.* B **61** 4222
[31] Gongora-T A, José J V, Schaffner S and Tiesinga P H E 2000 *Phys. Lett.* A **274** 117
[32] Moreira E S Jr 1998 *Phys. Rev.* A **58** 1678
[33] Ballentine L E 1998 *Quantum Mechanics: A Modern Development* (Singapore: World Scientific) chapter 7.3
[34] Makowski A J and Górska K J 2007 *Phys. Lett.* A **362** 26
[35] Goldin G A and Sharp D H 1983 *Phys. Rev.* D **28** 830
[36] Bose S K and Gupta N 1998 *Nuovo Cimento* B **113** 299
[37] Song X 1979 *J. Phys. G: Nucl. Phys.* **17** 49
Stillinger H 1979 *J. Math. Phys.* **20** 1891